

The effect of Sn addition on structure and glass transition temperature in Pb-Ge–Se chalcogenide glass

VIVEK MODGIL*, V. S. RANGRA

Department of Physics, Himachal Pradesh University Summerhill Shimla -171005, India

Infrared spectroscopy of the quaternary Sn added lead germanate chalcogenide glasses have been carried out in the far infrared spectral range 30cm^{-1} - 600cm^{-1} at room temperature. Glass transition temperature is decreasing as Sn concentration increases. FIR results support the variation of T_g and theoretically reported results. For all samples, FIR spectra show strong absorption peaks around 112cm^{-1} , 118cm^{-1} and 158cm^{-1} due to $\text{Sn}(\text{Se}_{1/2})_4$. A shift in absorption peaks towards high frequency is observed as x varies from 8 to 11. The absorption peaks appear around 197cm^{-1} for x=8, 12 which are due to GeSe_4 and bands around 176cm^{-1} , 185cm^{-1} due to GeSe_2 (Raman mode). Here Sn atoms appear to substitute for the germanium atoms in the outtrigger sites of $\text{Ge}(\text{Se}_{1/2})_4$ tetrahedra up to x=11 as it is reflected in the decrease in absorption bands of $\text{Ge}(\text{Se}_{1/2})_4$. With increasing Sn content from x=9 to 11 the reduction in polymeric rings of Se are observed as there is reduction in corresponding absorption bands of Se rings. At x =8, 12 the glasses show a vibrational band of an isolated F_2 mode of the Ge-centered tetrahedra outside the clusters. The absorption bands around 127cm^{-1} , 134cm^{-1} , 140cm^{-1} , 150cm^{-1} are due to Pb-Se which shifts to high frequency as aspect ratio of Pb-Se varies. The comparatively low bond energies of Pb-Se, Sn-Se than Ge-Se bond and strain effects of Pb, Sn are responsible for decreasing mean bond energy and glass transition temperature. The concentration dependence of the strong FIR features are consistent with that predicted by a network of fourfold-(twofold-) coordinated Sn(Se) and Ge(Se) atoms, with heteropolar bonds favored over homopolar bonds.

(Received September 13, 2012; accepted February 20, 2013)

Keywords: Quaternary chalcogenide glasses, Far infrared spectroscopy, Glass transition temperature

1. Introduction

In the material science one of the fundamental problems is to understand the relationship between the structure and observed macroscopic material properties and the nature of the microscopic structure of glass materials. Infrared spectroscopy is one of the most powerful and versatile analytical technique to understand the bonding structure of the amorphous materials. An understanding of the structure of an amorphous material is essential to understand its physical properties. Determining the structure is difficult for two main reasons. First, unlike for the crystal, there is no direct probe, such as X-ray diffraction, that can determine the structure of a glass uniquely. This is due to the absence of long-range order in the glass. Secondly, the glass may be in one of many possible metastable states and these states consist of different atomic configurations which may differ only slightly from one another and results in physical properties very similar to one another. The particular state in which a glass resides depends upon its parameters such as sample size, quenching and heating rates and the temperature from which it is quenched. As we know chalcogenide glasses contains S, Se or Te which constitute a rich family of vitreous semiconductors. Their properties can be modified as per the requirement of applications by using the suitable dopants.

Chalcogenide glasses are of wide-ranging importance in a variety of technological applications such as in the

areas of photonics and telecommunications[1,2] The unique compositional flexibility of these glasses in the form of continuous alloying enable tuning of optical, electronic, thermo-mechanical and other properties via compositional “engineering”. By introducing Sn and Te to Ge-Se glasses we expect to affect both the impurity peak of Ge-O as well as the multiphonon peaks and thus to improve the optical absorption of Ge-Se glasses near $10.6\mu\text{m}$ [3]. The Ge-O peak of contamination might be replaced by Sn-O. These impurity peaks rises due to thermodynamic stability of the oxides in the melt at the reaction temperature and the relative ratio between the elements.

Here in the present study, we report the far infrared absorption and variation of T_g in Pb, Sn doped Ge-Se type chalcogenide glasses $\text{Pb}_9\text{Se}_{71}\text{Ge}_{20-x}\text{Sn}_x$ (where x = 8, 9, 10, 11, 12 at. %). These studies are quite important as these lead to an insight in to the molecular structure and helps to understand the physical properties of these glasses.

2. Experimental study

Material synthesis and characterization: - The chalcogenide materials $\text{Pb}_9\text{Se}_{71}\text{Ge}_{20-x}\text{Sn}_x$ (where x = 8, 9, 10, 11, 12 at. %) are prepared by the melt quenching technique. Granules of Pb, and powder of Sn, Ge and Se having 99.999% purity are used. The material is then sealed in evacuated ($\sim 10^{-5}$ Torr) quartz ampoule (length ~

5 cm and internal diameter ~ 8 mm). The ampoules containing material are heated to 1000 °C and held at that temperature for 10 hours. The temperature of the furnace is raised slowly at a rate of 3 - 4° C per minute. During heating, the ampoule is constantly rocked, by rotating a ceramic rod to which the ampoule is tucked away in the furnace. This is done to obtain homogeneous alloy. After rocking for about 10 hours, the obtained melt is quenched in ice cool water. The quenched sample is then taken out by breaking the quartz ampoule and grinded to the fine powder. The nature of the material is ascertained by powder X-ray diffraction technique. For this, X-ray diffraction (XRD) patterns of sample are taken at room temperature by using an X-ray diffractometer Panalytical X'pert Pro (PW 3050/60). The copper target is used as a source of rays with $\lambda = 1.54 \text{ \AA}$ ($\text{CuK}_{\alpha 1}$). Material is amorphous in nature as there are no prominent peaks in the diffractograms shown in Fig. 2.1.

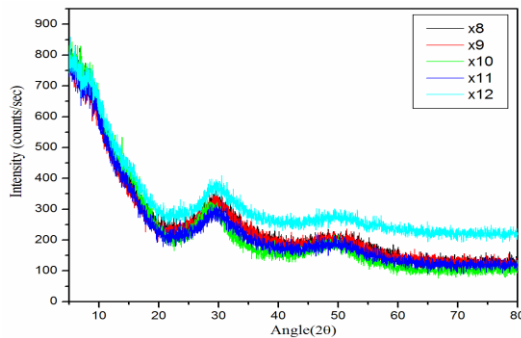


Fig. 2.1. X- Ray Diffractograms of the chalcogenide compositions $\text{Pb}_9\text{Se}_{71}\text{Ge}_{20-x}\text{Sn}_x$ (where $x = 8, 9, 10, 11, 12$).

Infrared spectra: The far-infrared spectra of different glassy alloys are recorded in the spectral range of 30cm^{-1} - 600cm^{-1} at room temperature using Perkin Elmer 1600 FT-IR Spectrometer with a resolution of 2 cm^{-1} . All the measurements were carried out using polythene pallet method. Powdered samples of 4 mg are thoroughly mixed and grinded with polythene after which the mixtures are pressed at 10 tons cm^{-2} for 5 min under vacuum. For the absorption of polythene, the spectrum of polythene is used

as a reference spectrum and then the spectrum of sample is divided by the reference spectrum to nullify the polythene absorptions.

Differential Scanning calorimetry: - DSC has been carried out on approximately 20 mg quantity of each powdered samples by DSC instrument Mettler Star SW 9.01 model in order to find the glass transition temperature at $10^\circ\text{C}/\text{minute}$ heating rate.

3. Results and discussions

A) Theoretical calculations of bond energy and relative bond formation

The properties of Pb-Ge-Se glassy system can be modified by the addition of metallic impurities. This addition has a pronounced effect on the structure of Ge-Se network. In selenium based chalcogenide glasses the metallic atoms play a dual role as network modifiers in Se rich side and network formers in Se deficient side and changes the properties considerably [4]. The probabilities of heteropolar bonds formation are greater as compared to homopolar bonds as is also evident from the bond probability calculations. The bond energy of heteropolar bonds can be calculated by the method suggested by Pauling using the bond energy of homopolar bonds and the electronegativity of the atoms involved. Bond energies of heteronuclear bonds are given by

$$D(\text{A-B}) = [D(\text{A-A}) D(\text{B-B})]^{1/2} + 30 (\chi_{\text{A}} - \chi_{\text{B}})^2 \quad (1)$$

Where $D(\text{A-B})$ = bond energy of heteronuclear bond, $D(\text{A-A})$ and $D(\text{B-B})$ are the bond energies of homonuclear bonds. χ_{A} and χ_{B} are the electronegativity values of A and B, respectively [5]. The electronegativity for Se, Ge, Sn and Pb are 2.55, 2.01, 1.96 and 2.33 respectively [6, 7]. The bond energies of the homopolar and heteropolar bonds and relative probabilities of different bonds are given in Table 3.1(a). Probabilities are calculated by using the probability function $e^{D/k_{\text{B}}T}$ at room temperature, where D is the bond energy, k_{B} is the Boltzmann constant and T is temperature [8].

Table 3.1(a). Bond energies and relative probabilities of bonds formation of possible bonds in material.

Bond	Bond Energy (Kcal/mol)	Rel. Bond Probability at 298.15K
Se-Ge	49.41	1
Se-Sn	49.23	7.3×10^{-1}
Se-Se	44.00	1.04×10^{-4}
Ge-Ge	37.60	2.03×10^{-9}
Se-Pb	31.47	6.2×10^{-14}
Pb-Pb	20.48	5.6×10^{-22}

B) Glass Transition Temperature (T_{g}): Experimentally measured T_{g} and T_{p} and theoretical calculated mean bond energy (shown in Table 3.1(b)) are

found to decrease as concentration of Sn increases. Fig. 3.1 shows the DSC thermograms of the material and inset shows the variation of T_{g} with increasing Sn concentration

This may be due to Sn atoms which have only a medium range interaction with the Ge atoms in the liquid state and take the fourfold coordination in the glassy state to form $\text{SnSe}_{4/2}$ tetrahedra units [4].

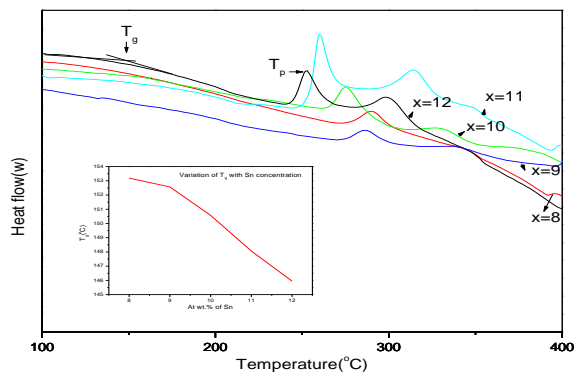


Fig. 3.1. DSC thermograms of the samples and variation of the T_g with Sn concentration.

Table 3.1(b). The glass transition temperature, crystallization temperature and mean bond energy (theoretical) of $\text{Pb}_9\text{Se}_{71}\text{Ge}_{20-x}\text{Sn}_x$ ($x = 8, 9, 10, 11, 12$ at. %).

Composition	Glass Transition Temperature(T_g) $^{\circ}\text{C}$	Peak Crystallization Temperature(T_p) $^{\circ}\text{C}$	Mean bond energy(<E> Theoretical)Kcal/mol
$\text{Pb}_9\text{Se}_{71}\text{Ge}_{12}\text{Sn}_8$	153.19	289.29	53.21
$\text{Pb}_9\text{Se}_{71}\text{Ge}_{11}\text{Sn}_9$	152.57	285.05	53.20
$\text{Pb}_9\text{Se}_{71}\text{Ge}_{10}\text{Sn}_{10}$	150.57	277.85	53.19
$\text{Pb}_9\text{Se}_{71}\text{Ge}_9\text{Sn}_{11}$	148.06	263.57	53.18
$\text{Pb}_9\text{Se}_{71}\text{Ge}_8\text{Sn}_{12}$	145.95	255.35	53.17

Thus, addition of Sn,Pb introduces strain to the network and leads to a considerable weakening of the Ge-Se network structure, this is reflected in the decrease of both the *mean bond energy and glass transition temperature* with increasing Sn content, as also reported earlier in our previous work of theoretical study of physical parameters [9]. The comparatively low bond energies of Pb-Se,Sn-Se than Ge-Se bond and strain effect of Pb,Sn are responsible for decreasing mean bond energy and glass transition temperature. The GeSe glass is composed of large clusters, larger than the clusters formed in GeSe_4 glass, the medium-range order tends towards long-range order, and the glass forming tendency is low compared to GeSe_4 . Further addition of Sn to the present network is difficult if the glassy state is to be maintained because further at $x=13$ material become crystalline.

C) Infrared spectroscopy

C.1 Qualitative studies

The absorption bands in the present chalcogenide glasses are appearing in the far infrared region 30-600

There is an isomorphous replacement of Ge atoms by Sn atoms in the glass network; thus Sn atoms are incorporated into the clusters of Ge-Se alloys. The tetravalent Sn, which combines only with Se, has a covalent radius of 1.41 Å, 15% larger than the covalent radius of Ge(1.22Å), Pb has covalent radii 1.46 Å which is also greater than Ge. So Pb-Se, Sn-Se bonds has a larger ionicity than the Ge-Se bond, which causes lack of flexibility of the bond angles between Se and Sn,Pb atoms.

cm^{-1} . The far infra-red spectra of the $\text{Pb}_9\text{Se}_{71}\text{Ge}_{20-x}\text{Sn}_x$ (where $x = 8, 9, 10, 11, 12$ at. %) material are discussed under the following assumptions: (i) The 'valence force field model' (VFF) [10] (ii) The position of the intrinsic IR features is influenced mainly by stretching force constants of corresponding bonds formed in the material. The wavenumbers of the vibrational modes in the far infrared region are determined by the masses of the atoms and the interatomic forces within the bonds of the atoms present in amorphous network. The wavenumber ν is given by the following formula

$$\nu = \frac{1}{2\pi c} \left(\frac{k}{\mu} \right)^{1/2} \quad (2)$$

where k is the force constant of the bond and c is the speed of light.

μ is the reduced mass of the molecule/bond which is given by

$$\mu = \frac{M_1 M_2}{M_1 + M_2} \quad (3)$$

where M_1 and M_2 are the atomic masses of the two atoms. There are number of authors who gave the relationships to

calculate the force constant K_r (i) According to Gordy[11] the force constant can be calculated as

$$k_r = aN \left(\frac{\chi_a \chi_b}{d^2} \right)^{3/4} + b \quad (4)$$

This relation holds accurately for a large number of diatomic and simple polyatomic molecules in their ground states. Here, a and b are constants which depend on the structural unit type, d is the bond length, χ_a and χ_b are the electronegativities in the Pauling scale and N is the bond order, which can be determined from the expression

$$N = \frac{d + 2r_1 - 3r_2}{2d + r_1 - 3r_2} \quad (5)$$

where r_1 and r_2 are the covalent radii for the single and double bond, respectively. (ii) Somayayulu [12] has developed a method for predicting the polyatomic force constants by using the elemental covalent force constants and electronegativities as

$$k_{AB} = (k_{AA} k_{BB})^{1/2} + (\chi_A - \chi_B)^{1/2} k_{AB} \quad (6)$$

Here k_{AB} is the force constant between the elements A and B, and k_{AA} and k_{BB} are the force constants for bonds A-A and B-B, respectively, the values of which are (10^5 dyn cm^{-1}) 1.29 for Ge-Ge, 1.21 for Sn-Sn, 0.8 for Pb-Pb [13] and 1.91 for Se-Se. Bond-stretching forces acting as mechanical constraints are present in Ge, Se, Pb and Sn. Bond bending constraints are important in Ge and Se but may be ignored in Sn and Pb because the corresponding force constant are weak compared to Ge and Se[14]. The force constants, bond lengths and reduced mass of possible bonds are shown in Table 4.1.

Table 4.1. Various bonds possible in material with their reduced mass, bond length and force constants.

Bond	Reduced mass 10^{-26} (KgU ⁻¹)(μ)	Bond length (nm)(d)	Force Constant K_{AB} (eV)
Ge-Ge	6.060	0.245	1.29
Ge-Sn	7.513	0.262	1.25
Ge-Pb	8.92	0.298	1.02
Ge-Se	6.301	0.239	1.93
Pb-Se	8.82	0.291	1.24
Pb-Sn	12.53	0.315	0.99
Pb-Pb	17.20	0.350	0.80
Sn-Se	7.884	0.257	1.52
Sn-Sn	9.882	0.280	1.21
Se-Se	6.559	0.232	1.91

The basic information about the atomic configuration of the glasses in amorphous state can be obtained from comparing the IR spectra of the amorphous state of the glasses with their crystalline analogues. On comparing the IR spectra of both states it is found that the basic structural units in the glasses are essentially the same as those in the corresponding crystalline material. In the structure of chalcogenide glasses, according to chemical bond approach, [8] priorities of heteropolar bonds formation are greater over the homopolar bonds and the bonds are formed in order of decreasing bond energy until all the available valences of the atoms are satisfied.

C.2 Quantitative justification of some absorption bands

In the present chalcogenide glasses, various absorption bands are appearing in the far infrared region 30-600 cm^{-1} as shown in the Fig. 5.1 and tabulated in the Table 5.1. The infrared spectra of the Ge based amorphous chalcogenide semiconductor have been largely interpreted in terms of the vibrations of the isolated molecular units in such a way as to preserve the fourfold and two fold coordination for Ge, Sn and chalcogen atoms respectively. Different models have been suggested to explain structure of chalcogenide glasses such as chain crossing model (CCM) of Tronc et al [15] and the random covalent network model (RCNM) of Lecovsky et al [16]. The chemically ordered network model (CONM) is also used to explain the structure of the vitreous material, according to this heteropolar bonds are preferred over homopolar bonds and they are formed in order of their decreasing bond energies [17]. From Raman scattering studies, it has been realized that the local structure of Ge-Se glasses consists of chain segments of *edge-sharing* GeSe_2 and *corner-sharing* GeSe_4 tetrahedra. Glasses possess the random covalent structure according to covalent network model (RCNM) of Lucovsky et al [16]. In selenium based chalcogenide glasses the metallic atoms play a dual role as network modifiers in Se rich side and network formers in Se deficient side change the properties considerably [4]. We have observed all possible heteropolar bonds of Pb, Sn and Ge with Se in the FIR spectrum.

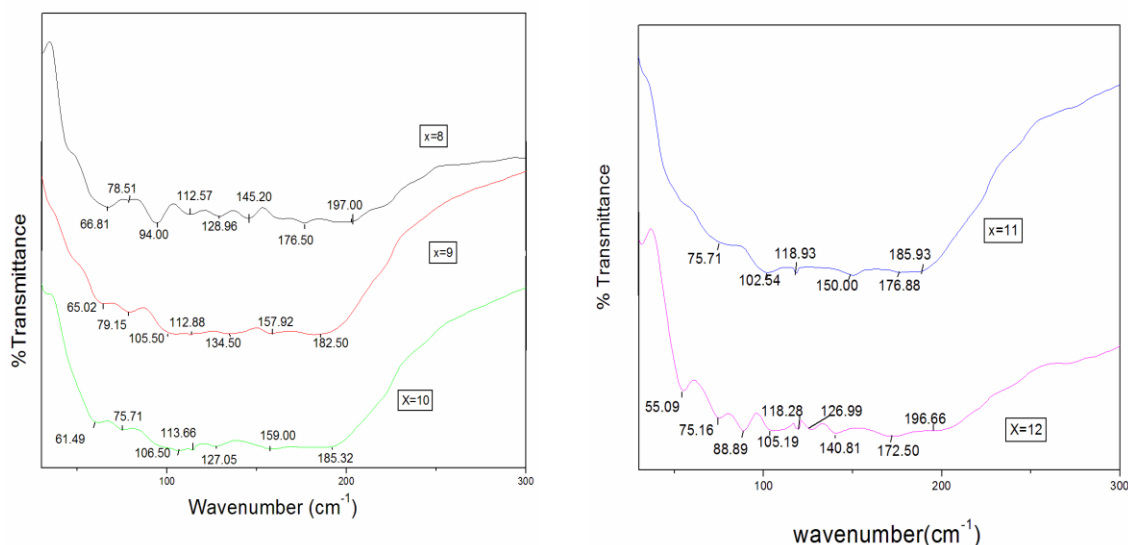


Fig 5.1(a),(b). FIR spectrum of $Pb_9Se_{71}Ge_{20-x}Sn_x$ ($x = 8, 9, 10, 11, 12$ at. %).

In the first sample at $x=8$ the absorption bands 65cm^{-1} - 95cm^{-1} are due to the Se_8 (E_2 mode) [18] while the bands 102cm^{-1} - 106cm^{-1} has been assigned to infrared active A_2 mode of trigonal Selenium. According to Oshaka [19] an infrared active fundamental mode in the spectra of Se containing Te at 102cm^{-1} is due to A_2 mode of trigonal selenium. The shoulders at $58\text{--}88\text{cm}^{-1}$ and 121cm^{-1} can be considered as Se_8 rings, These polymeric rings reduces as there are number of absorption peaks in corresponding

band reduces when x varies from 8 to 11. This is due to increase in concentration of Sn as it produces more attacking sites to form heteropolar bonds. The bands at 112.57cm^{-1} , 112.88cm^{-1} , 113.66cm^{-1} , 118.28cm^{-1} are due to $Sn(Se_{1/2})_4$ which shifts to the high frequency side as the x varies from $x=8$ to $x=12$ which depicts that heteropolar bonds of Sn with Se increase.

Table 5.1. FTIR spectrum peak assignments to various possible bonds in $Pb_9Se_{71}Ge_{20-x}Sn_x$ ($x = 8, 9, 10, 11, 12$ at. %).

S.No	X=8	X=9	X=10	X=11	X=12	Assignments
1.	66.81	65.02	61.49		55.09	Se_8 (E_2 mode)
2.	78.15	79.15	75.71	75.71	75.16	Se_8 (E_2 mode)
3.	94.00	-			88.89	Se_8 (E_2 mode)
4.	--	105.50	106.50	102.54	105.19	Trigonal Se (A_2 mode)
5.	112.57	157.92, 112.88	159.00, 113.66	118.93	118.28	$Sn(Se_{1/2})_4$
6.	128.96, 145.20	134.50	127.05	150.00	126.99, 140.81	Pb-Se
7.	176.50	182.50	185.32	176.88, 185.93	172.50	$GeSe_2$ (Raman mode)
8.	197.00				196.66	$GeSe_4$

With further addition of Sn, the band (112cm^{-1}) remains but becomes broader and shifts toward high frequency side [20,21]. The bands at 157.92cm^{-1} , 159.00cm^{-1} for $x=9, 10$ are due to $Sn(Se_{1/2})_4$. The absorption bands

176.50cm^{-1} at $x=8$, 176.88cm^{-1} , 172.50cm^{-1} at $x=11, 12$ respectively and 182.50cm^{-1} , 185.32cm^{-1} , 185.93cm^{-1} at $x=9, 10, 11$ respectively are due to the formation of the $GeSe_2$ Raman mode [6,22]. However some absorption

peaks are observed at higher frequency 197cm^{-1} due to the GeSe_4 at $x=8,12$ [23]. In the FIR spectrum there are absorption bands $128.96\text{ cm}^{-1}, 145.20\text{ cm}^{-1}$ at $x=8,134.50\text{ cm}^{-1}$ at $x=9,127.05\text{ cm}^{-1}, 150.00\text{ cm}^{-1}$ at $x=10,11$ respectively and $126.99\text{ cm}^{-1}, 140.81\text{ cm}^{-1}$ at $x=12$ which are due to Pb-Se bonds. For $x=11, 12$ this band shifts towards high frequency side $140\text{ cm}^{-1}, 145\text{ cm}^{-1}, 150\text{ cm}^{-1}$.

For $x=8, 10$ it shifts towards low frequency side. The asymmetric splitting of peaks at $x=8, 12$ are due to change in the aspect ratio of Pb with Se [24-28]. Lead chalcogenides formed are usually ionocovalent and Pb atoms exist in Pb^{2+} state. This nature is due to strong polarizability of lead and large difference in electronegativity between Pb and chalcogenides. In Pb-Ge-Se glasses Pb atom transfer an electron to a C_3^+ centre and modifies into a C_2^0 centre. Simultaneously it also creates C_1^- centre by donating another electron to adjacent C_2^0 site. There is resultant ionic bonding between the Pb^{2+} ion and the C_1^- and C_2^0 centers created [29].

In $\text{Pb}_9\text{Se}_{71}\text{Ge}_{20-x}\text{Sn}_x$, Sn atoms are supposed to replace the Ge atoms in the 'outrigger' sites. With increase in the Sn concentration, the scarcity of these sites causes the 'rafts' to break up into smaller 'rafts', creating more 'outrigger' sites for the Sn atoms to occupy. In $\text{Pb}_9\text{Se}_{71}\text{Ge}_{20-x}\text{Sn}_x$ glasses, the substitution of Ge atoms by Sn atoms takes place up to $x=12$. As a result of this the number of the $\text{Ge}(\text{Se}_{1/2})_4$ bands decrease with the increase in concentration x whereas the number of the $\text{Sn}(\text{Se}_{1/2})_4$ bands increase. The shift of peaks in the spectrum is attributable to the presence of a $(\text{SnSe}_{1/2})_4$ tetrahedron unit, when concentration of Sn increases, intercluster interaction results in softening of the breathing mode and shifting in the polarizability of the structure [30]. The relative probability of bond formation shows the least existence of homopolar bonds which is in good agreement with the Far-infrared spectra results. In the glassy state Sn form $\text{SnSe}_{4/2}$ tetrahedra units with Se. There is an isomorphous replacement of Ge atoms by Sn atoms in the glasses network; thus Sn atoms are incorporated into the clusters of Ge-Se alloys [31, 32]. The covalent radii of Pb, Sn are larger than the covalent radii of Ge which increases ionic character of Pb-Se and Sn-Se bonds. This causes lack of flexibility of the bond angles between Se and Sn atoms. Thus, addition of Sn, Pb introduces strain to the network and leads to a considerable weakening of the Ge-Se network structure. This is indicated by the decrease of mean bond energy and T_g with increasing Sn concentration.

4. Conclusions

FIR measurements have been performed on a series of well characterized $\text{a-Pb}_9\text{Se}_{71}\text{Ge}_{20-x}\text{Sn}_x$ glassy systems in the concentration range ($x=8, 9, 10, 11, 12$). The results are interpreted in terms of the vibrations of the isolated molecular units in such a way as to preserve fourfold and twofold coordination for germanium, tin and chalcogen atoms, respectively. The theoretically calculated mean bond energy and experimental analysis of far-infrared

spectrum agree with the CCM and chemical bond approach model. We see the bands due to Se rings, Sn-Se, Ge-Se and Pb-Se bonds in our FIR spectra. The effect of increasing concentration of Sn causes the 'rafts' to break in to the smaller one and create the more outrigger sites for Sn to occupy and substitute the Ge which is also reflected in decrease in the number of absorption bands due to Se_8 polymeric rings and Ge-Se bonds. The decrease in the T_g with increasing Sn concentration is due to increasing concentration of Sn-Se bonds in the glassy network which is also evident from our FIR results. The comparatively lower bond energies of Pb-Se and Sn-Se bonds than Ge-Se bond and strain effects of the Pb, Sn atoms in the network weaken the glassy structure and causes a decrease in the glass transition temperature and mean bond energy of this chalcogenide material.

References

- [1] A. Zakery, S. R. Elliott, J. Non-Cryst. Solids, **330**, 1 (2003).
- [2] K. Shimakawa, A. V. Kolobov, S. R. Elliott, Adv. Phys. **44**, 475 (1995).
- [3] I. Haruvi-Busnach, J. Dror, N. Croitoru, J. Mater. Res., **5**(6), 1215 (1990).
- [4] B. J. Madhu, H. S. Jayanna, S. Asokan Eur. Phys. J. B **71**, 21 (2009).
- [5] A. Dahshan, K. A. Aly, Phil. Mag., **88**(3), 361 (2008).
- [6] L. Pauling, The Nature of the Chemical Bond, Cornell University Press, New York, (1960).
- [7] A. K. Pattanaik, A. Srinivasan, Semicond. Sci. Technol. **19**, 157 (2004).
- [8] Jozef Bicerano, Stanford R. Ovshinsky, J. Non-Cryst. Solids **74**, 75(1985).
- [9] Vivek Modgil, V. S. Rangra J. Optoelectron. Adv. Mater. **13**(2), 158 (2011).
- [10] L. Tichy, H. Ticha, A. Pacesova, J. Petzelt, J. Non-Cryst. Solids **128**, 191(1991).
- [11] W. Gordy, J. Chem. Phys. **14**(5), 305 (1946).
- [12] G. R. Somayayulu, J. Chem. Phys. **28**(5) 814 (1958).
- [13] Khaled Toukan, H. T. J. Reijers, C. K. Loong, L. Price David, and Saboungi Marie-Louise Phy Rev. B 3rd, **41**, 17 (1990).
- [14] S. A. Fayek, Infrared Physics & Technology **46**, 193 (2005).
- [15] Tronc, M. Bensoussan, A. Brenac, C. Sebenne, Phys. Rev. B **8**, 5947, (1973).
- [16] G. Lucovsky, F. L. Galeener, R. C. Keezer, R. H. Geils, H. A. Six, Phys. Rev. B **10**(12), 5134 (1974).
- [17] S. R. Elliot, Physics of Amorphous Solids, Longman Inc, New York, 134, (1984).
- [18] G. J. Ball, J. M. Chamberlain, J. Non-Cryst. Solids **29**, 239 (1978).
- [19] T. Oshaka, J. Non-Cryst. Solids **17**(1), 121 (1975).
- [20] Rajneesh Kumar, Parikshit Sharma, S. C. Katyal, Pankaj Sharma, V. S. Rangra, J. Appl. Phys. **110**, 013505 (2011).
- [21] Adam Abdallah Belal Journal of King Saud University (Science) **21**, 93 (2009).

- [22] S. C. Katyal, R. C. Verma, *J. Phys.: Condens. Matter* **5**, 3469 (1993).
- [23] D.R. Goyal, A. S. Maan, *J. Non-cryst. solids*, **183**, 182 (1995).
- [24] F. S. Manciu, Y. Sahoo, F. Carreto, P. N. Prasad, *J. Raman Spectrosc.* **39**, 1135 (2008).
- [25] S. V. Ovsyannikov, Y. S. Ponosov, V. V. Shchennikov, V. E. Mogilenskikh, *phys. stat.sol.(c)* **1**, No. 11, 3110–3113 / DOI 10.1002/pssc.200405280 (2004).
- [26] Byung-Ryool Hyun, A. C. Bartnik, Weon-kyu Koh, N. I. Agladze, J. P. Wrubel, A. J. Sievers, Christopher B. Murray, W. Wise Frank, *Nano Lett.*, **11**, 2786 (2011)
- [27] H. R. Chandrasekhar, R. G. Humphreys, U. Zwick, M. Cardona, *Phy. Rev. B* **15**(4), 2177 (1977).
- [28] L. K. Vodop'yanov, L. A. Falkovskii, J. Irvin, S. Himenis, *JETP Lett.* **53**, 561 (1991).
- [29] S. Murugavel, S. Asokan, *Phy. Rev. B* **58**(8), 4449 (1998).
- [30] L. E. McNeil, J. M. Mikrut, M. J. Peters, *Solid State Commun.* **62**(2), 101 (1987).
- [31] T. Fukunaga, Y. Tanaka, K. Murase, *Solid State Commun.* **42**, 513 (1982).
- [32] B. P. Boolchand, M. Stevens, *Phys. Rev. B* **29**, 1 (1984).

*Corresponding authors: vivekmodgilphysics.hpu@gmail.com
vs_rangra@yahoo.co.in